



HAL
open science

Recent results from the INDRA Collaboration

N. Le Neindre, G. Adémard, L. Augey, Eric Bonnet, B. Borderie, R. Bougault,
A. Chbihi, Q. Fable, J.D. Frankland, E. Galichet, et al.

► **To cite this version:**

N. Le Neindre, G. Adémard, L. Augey, Eric Bonnet, B. Borderie, et al.. Recent results from the INDRA Collaboration. International Workshop on Multi facets of EoS and Clustering, May 2016, Caen, France. pp.377, 10.1393/ncc/i2016-16377-7 . hal-02058512

HAL Id: hal-02058512

<https://hal.science/hal-02058512>

Submitted on 8 Mar 2019

HAL is a multi-disciplinary open access archive for the deposit and dissemination of scientific research documents, whether they are published or not. The documents may come from teaching and research institutions in France or abroad, or from public or private research centers.

L'archive ouverte pluridisciplinaire **HAL**, est destinée au dépôt et à la diffusion de documents scientifiques de niveau recherche, publiés ou non, émanant des établissements d'enseignement et de recherche français ou étrangers, des laboratoires publics ou privés.

Recent results from the INDRA Collaboration

N. LE NEINDRE⁽¹⁾, G. ADÉMARD⁽²⁾⁽³⁾, L. AUGÉY⁽¹⁾, E. BONNET⁽²⁾,
B. BORDERIE⁽³⁾, R. BOUGAULT⁽¹⁾, A. CHBIHI⁽²⁾, Q. FABLE⁽²⁾, J.D. FRANKLAND⁽²⁾,
E. GALICHET⁽³⁾⁽⁴⁾, D. GRUYER⁽²⁾, M. HENRI⁽¹⁾, O. LOPEZ⁽¹⁾, P. MARINI⁽²⁾,
M. PÂRLOG⁽¹⁾, M. F. RIVET^{(3)†}, E. ROSATO^{(5)†}, G. VERDE⁽³⁾, E. VIENT⁽¹⁾
and M. VIGILANTE⁽⁵⁾⁽⁶⁾ for the INDRA COLLABORATION

- ⁽¹⁾ *LPC Caen, Normandie Univ, ENSICAEN, UNICAEN, CNRS/IN2P3, LPC Caen - 14000 Caen, France*
⁽²⁾ *GANIL, CEA/DSM-CNRS/IN2P3 - B.P. 5027, F-14076 Caen cedex, France*
⁽³⁾ *Institut de Physique Nucléaire, CNRS/IN2P3, Université Paris-Sud 11 - F-91406 Orsay cedex, France*
⁽⁴⁾ *Conservatoire National des Arts et Métiers - F-75141 Paris cedex 03, France*
⁽⁵⁾ *INFN, Sezione di Napoli - Complesso Universitario di Monte S. Angelo, via Cinthia, 80126 Napoli, Italy*
⁽⁶⁾ *Dipartimento di Fisica, Università di Napoli "Federico II" - Complesso Universitario di Monte S. Angelo, via Cinthia, 80126 Napoli, Italy*

received 10 January 2017

Summary. — In this conference proceeding we introduce the last results obtained by the INDRA Collaboration. Those results will be better explained and more detailed in the following report presentations of this issue and just a brief overview will be mentioned here, with only the main conclusions addressed. This summary is divided into two parts. The first one is devoted to systematic studies on heavy-ion collisions around Fermi energy with the INDRA multidetector array. Analyses of nuclear reactions in term of dissipation, reaction mechanisms, decay modes, isospin diffusion, excitation energy and calorimetry will be discussed. This has been done thanks to the large INDRA data base, collected over most than twenty years now. The second part of this proceeding concerns analyses of data with a specific set-up: INDRA coupled with the VAMOS spectrometer. Complementary studies with full determination of all the particles event by event (Z, A, E, θ, ϕ) has been performed to access important parameters like symmetry energy, level density parameters, full decay channels (partitions), E^* , temperature which are the main ingredients in the decay of hot heavy ions.

† Deceased.

1. – Systematic studies on heavy-ion collisions with INDRA

The full INDRA data set for different systems and beam energies allows systematic studies of nuclear reactions in term of dissipation, reaction mechanisms, decay modes, isospin diffusion... In the very last studies performed by the whole collaboration many items have been addressed. Transport properties in nuclear matter around fermi energy (stopping and in-medium effects) [1], evaluation of the reaction and fusion cross sections with incident energy (evolution of the reaction mechanisms and their decay) [2], for the decay mechanisms, evolution of the time emission sequence by Coulomb chronometry [3], reaction mechanisms in 3-body central collisions of $^{129}\text{Xe}+^{nat}\text{Sn}$ at 8–15 A MeV [4], achievement of chemical equilibrium in central collisions with the same system and energy but with different isospin [5] and finally caloric curves [6].

In [1] by looking specifically at free nucleons (here protons), we present experimental results concerning the mean free path, the nucleon-nucleon cross-section and in-medium effects in nuclear matter. Indeed, with heavy-ion collisions around Fermi E , dissipation is related to the properties of the mean field. But when beam E increase NN collisions become important (less Pauli blocking). By determining the relative degree of proton nuclear stopping as a function of system mass and bombarding energy, we show that the stopping can be directly related to the transport properties in the nuclear medium. We apply this method on different systems and beam energies Gd/U+U, Ta/Au+Au, Xe+Sn, Ni+Ni, Ar+Ni, Ar+KCl. Some total mass effects are observed: the heavier the system, the higher the isotropy ratio is. This supports the fact that the stopping, *i.e.*, the conversion from longitudinal to transverse energy, is related to the number of participants in the system. The evolution of the in medium factor $F = \sigma_{NN}^{in-medium} / \sigma_{NN}^{free}$ for the nucleon-nucleon cross section in nuclear matter is presented in fig. 1. In-medium effects are quite important meaning a significant reduction of the $\sigma_{NN}^{in-medium}$: 80% at 35 A MeV and 50% at 100 A MeV. This energy dependence for the in-medium σ_{NN} has to be properly taken into account in any transport model. The next step in the future, is to perform the same analysis with radioactive beams to determine, if any, the isospin dependence of σ_{NN} .

We have seen that in-medium effects (which are related to transport properties) are important in nuclear matter and evolve with beam energy. In [2] we propose an overview of reaction mechanisms and fusion cross section determinations. Fusion reactions in $^{129}\text{Xe}+^{nat}\text{Sn}$ collisions for energies ranging from 8 A MeV to 35 A MeV are calculated. Starting from lower energies (8, 12, 18 A MeV) one observes events of fusion/fission and DIC (Deep Inelastic Collisions) which evolve toward instantaneous break up as the energy deposit increases. We evaluated the fusion/incomplete fusion for the incident energies from 8 to 35 A MeV by selecting classes of events corresponding to damped reactions (\sim main Z_i products in the CM) which are good candidates to fusion/quasi fusion. In these selections one can observe the formation of a composite system having roughly a velocity close to the centre-of-mass velocity for lower energies. As the available energy increases one assists at an evolution of the composite toward a more binary phenomena. Fusion and quasi fusion gradually become less probable, the reaction products are more and more emitted in the forward direction and the system, formed in a DIC fashion or in massive transfers, undergoes multiple fragmentation see fig. 2. (Note that probably at 8 and 12 A MeV the values of the cross sections are higher, at these energies the detector acceptance is suspected to be responsible for the loss of fusion/quasi fusion events since all the residues with small forward angle are lost).

In the previous analysis we observed a quite large amount of fusion/incomplete fusion

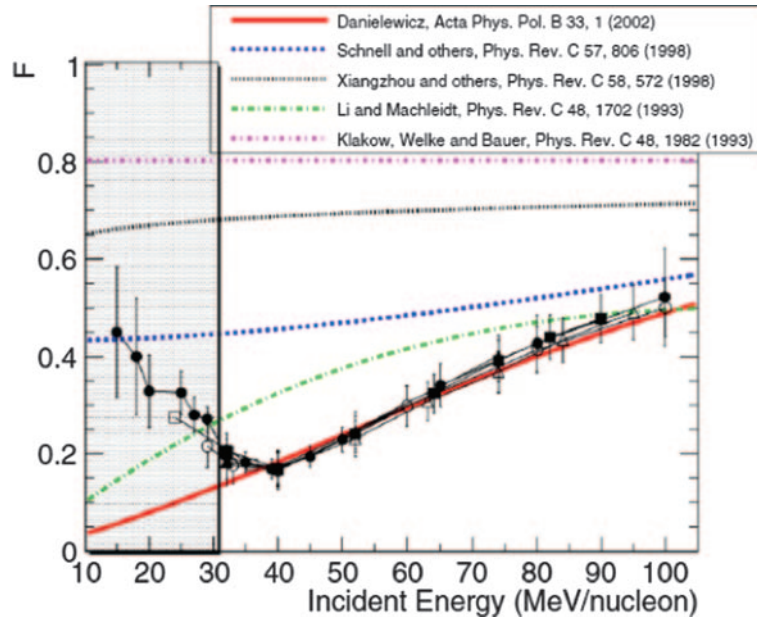


Fig. 1. – In-medium factor $F = \sigma_{NN}^{in-medium} / \sigma_{NN}^{free}$ for the nucleon-nucleon cross section in nuclear matter. The different curves correspond to some parametrizations used in transport models. See [1].

cross section for the system $^{129}\text{Xe} + ^{nat}\text{Sn}$ around 12–20 A MeV. Among these events the three-fragment exit channel occurs with a significant cross section, indeed it already outgrows the two-fragment exit channel at 18 and stay the most probable decay up to 32 A MeV. How are these events produced? Fusion-Fission? Quasi fission? Deeply

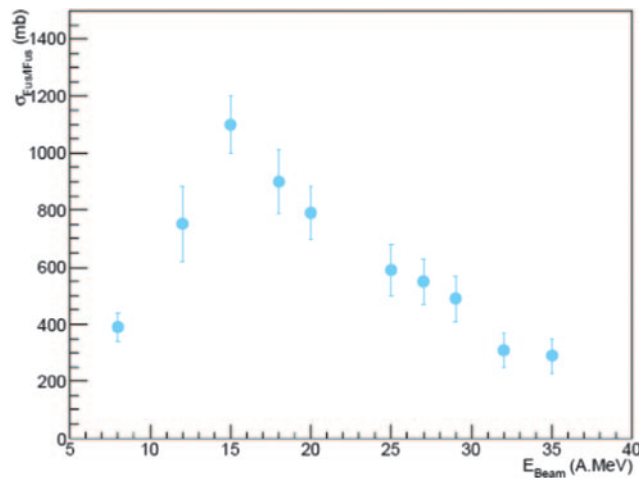


Fig. 2. – Fusion/Fission experimental cross section for the system $^{129}\text{Xe} + ^{nat}\text{Sn}$ from 8 to 35 A MeV. From [2].

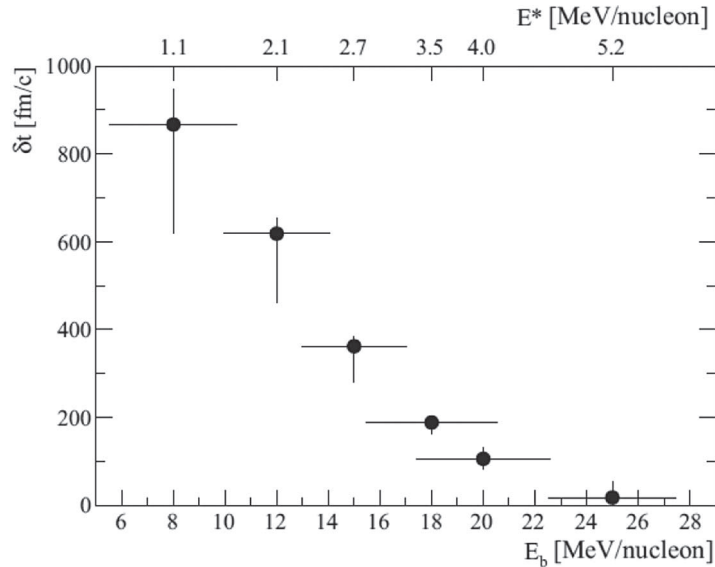


Fig. 3. – Evolution of the mean intersplitting time as a function of the beam energy (lower scale) and the estimated excitation energy of the initial composite systems (upper scale) produced in $^{129}\text{Xe}+^{nat}\text{Sn}$ central collisions. See [3].

inelastic collisions? Neck between QP and QT? In the analysis performed in [3] we show that these fragments arise from two successive binary splitting of a heavy composite system. The sequence of fragment production is determined. A strong asymmetry in the first splitting has been observed. Strong Coulomb proximity effects are observed in the three-fragment final state. We use a proximity parameter to get a time interval between splittings. A comparison with Coulomb trajectory calculations shows that the time scale between the consecutive breakups decreases with increasing bombarding energy, becoming quasi simultaneous, see fig. 3. This transition from sequential to simultaneous breakup was interpreted as the signature of the onset of multi fragmentation for the three-fragment exit channel in this system, which arises around 3 A MeV.

In [4] a deeper analysis tries to disentangle the different mechanisms responsible for the three-fragment exit channel previously studied and extract their respective cross sections. This is done thanks to comparison with calculations filtered by the experimental set-up and using the same criteria selection to reproduce the effects they (possibly) induce.

In the previous analyses we have studied the transport properties occurring in nuclear reactions around Fermi energy. The way it is related to the nucleon properties in nuclear medium, how it evolves with incident energy and system size. How it produces hot nuclear matter which then deexcites in different exit channels (peripheral collisions, deep inelastic collision, central collisions...). Among them we have analysed events leading to fusion quasi-fusion, extract their cross sections and followed some specific decays like the three fragments exit channel to extract some typical time sequences and their evolutions. Now we focus on another phenomena linked to the transport properties in nuclear matter which are the projectile/target nucleon exchange and chemical composition. Indeed the mid rapidity zone, produced in between the two interacting partners, is mainly governed by diffusion and drift isospin transport phenomena at this bombarding energy.

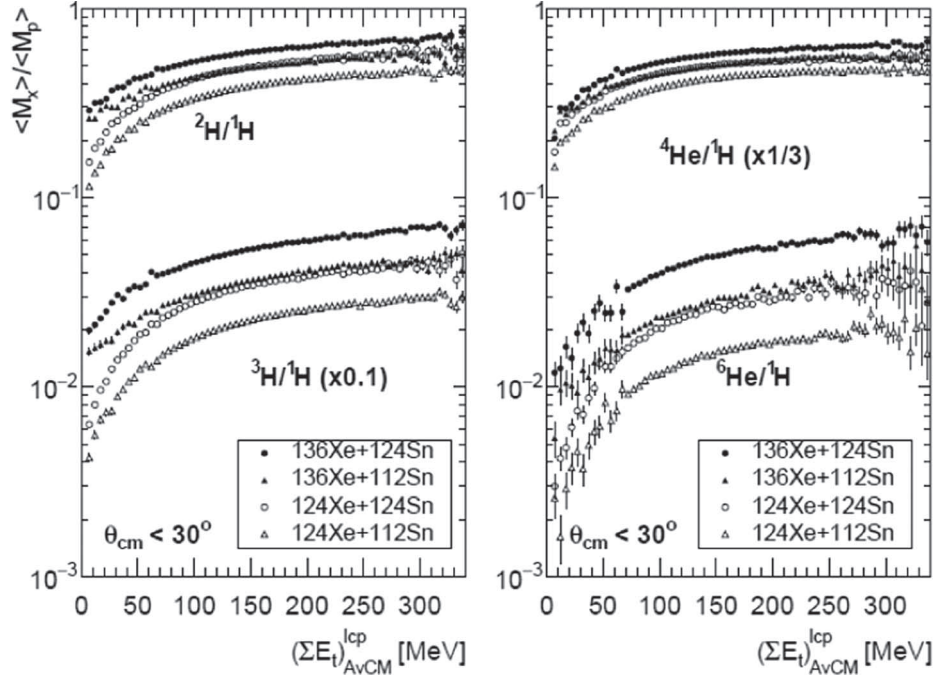


Fig. 4. – Forward centre-of-mass cluster abundance ratios for each studied reaction as a function of the impact parameter evaluator. From [5].

This study, more detailed in [5], is limited to the forward part of the centre of mass. It is thus focused on the evolution of projectile-like fragment isotopic content. The two studied reactions $^{124}\text{Xe}+^{124}\text{Sn}$ and $^{136}\text{Xe}+^{112}\text{Sn}$ were chosen to study the path towards chemical equilibrium since their projectile target combined systems are identical. Whereas the two other systems $^{136}\text{Xe}+^{124}\text{Sn}$ and $^{124}\text{Xe}+^{112}\text{Sn}$ give the most extreme combinations of high and low value of isospin. The evolution towards chemical equilibrium, if any, is sorted thanks to the transverse energy of light particles ($Z \leq 2$) in the centre of mass forward emisphere ($\sum E_t)_{AvCM}^{lcp}$. In order to take into account selection and set-up effects we compare cluster mean multiplicities relative to proton mean multiplicity (hereafter called cluster abundance ratios). Doing so, selection effects are (as far as we can) canceled and it is then possible to compare cluster abundance ratios whatever the impact parameter is. The use of cluster abundance ratios allows also to study chemical equilibration process because trivial size dependences are (hopefully) removed. In fig. 4 we observe that for $(\sum E_t)_{AvCM}^{lcp}$ greater than about 150 MeV, $^{124}\text{Xe}+^{124}\text{Sn}$ and $^{136}\text{Xe}+^{112}\text{Sn}$ system mean abundance ratios are almost the same. This global system N/Z dependence implies that chemical equilibrium is almost achieved for central collisions. For projectile-like de-excitation region (selected with $\theta_{CM} < 30^\circ$), the evolution starts from almost N/Z projectile dependence to N/Z total system dependence. For mid-rapidity region ($\theta_{CM} > 60^\circ$, not shown) the values are also projectile N/Z dependent for very peripheral reactions whereas they also reach a N/Z total system dependence for central collisions. This evolution reflects the drift/diffusion isospin phenomena.

In the last couple of years, a better estimation of the excitation energy, the so called 3D-calorimetry, was developed within the INDRA Collaboration, see [6]. Thanks to

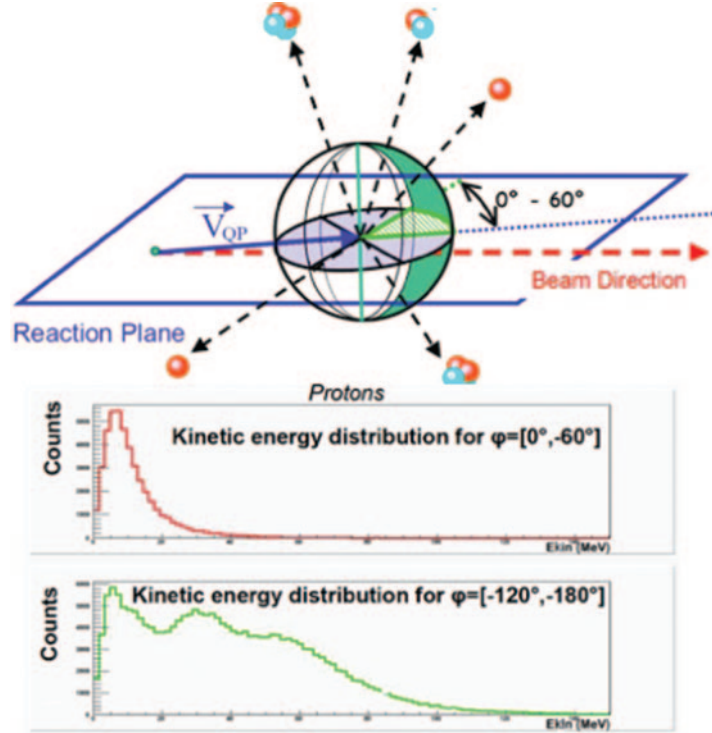


Fig. 5. – Above, definition of the ϕ angle used to separate different angular domains in the Quasi Projectile QP reference frame. Lower panel, two kinetic energy spectra obtained in two angular regions $\phi = [0^\circ, -60^\circ]$ and $\phi = [-120^\circ, -180^\circ]$ showing how “clean” is the reference one in red (in term of pure evaporation thanks to its Maxwellian shape) as compared to another one more polluted, green curve. From [6].

the improvements, over the last years, on the knowledge of time sequence and origin of particle emission, this new calorimetry try to overcome the difficulties coming from the different nature of emission (pre-equilibrium, sequential decay, multifragmentation, spin, angular distribution...) and based on close comparison with simulation by event generator (where all this information is known) suggests an accurate method to determine the amount of energy store in hot nuclei. An estimate of evaporation probability in all space according to the kinetic energy and the different angular domain by comparison with a reference domain (as free as possible from any other source of emission than evaporation from the Quasi-Projectile (QP) itself) is performed. On fig. 5 we can see two kinetic energy distributions associated to two different angular domains $\phi = [0^\circ, -60^\circ]$ and $\phi = [-120^\circ, -180^\circ]$ define on the scheme above. We see how “polluted” is the last one while the former has a very “Maxwellian shape” one, as expected in the case of pure evaporation. This domain, $\phi = [0^\circ, -60^\circ]$, is used as the reference one to define the evaporation probability $\text{Prob}_n(E_k, \theta, \phi, E_{LLCP})$ then use to estimate the QP size ($Z_{QP} = \sum \text{Prob}_n \times Z_n$ and A_{QP}) and its excitation energy event by event. With this new method a systematic study of the caloric curves, for Quasi-Projectile (QP) produced in dissipative events of different systems and incident energy, have been done, see [6] for more details on this subject.

2. – The INDRA-VAMOS experiments

The second part of this conference proceeding focus on a specific experimental set-up which coupled the VAMOS spectrometer and the INDRA multidetector. The goal of this campaign of measurements is to have access event by event to the mass and charge of fragments, produced in heavy ion collisions, together with the usual isotopic identification of light charged particles (LCP). Indeed, so far with 4π array, only the charge Z was solved. Mass determination open a new dimension since isotopic distribution of fragments are very usefull tools for symmetry energy observables as well as isospin physic studies in general.

Thanks to this powerfull device, allowing to reconstruct not only the charge Z but also the mass A of the quasi-projectile (QP) a specific analysis has been published recently [7]. It concerns signals of Bose Einstein condensation and Fermi quenching in the decay of hot nuclear systems. Knowing better the masses it has been demonstrated that while bosons seem to condense, experiencing higher densities and smaller relative distances, fermions, due to the Pauli principle, tend to move apart, experiencing lower densities and larger relative distances. Bosons experience higher local partial densities both in purely boson-like events and in mixtures of bosons and fermions. Those signals are consistent with the possible existence of Bose-condensation phenomena, which persist even in the presence of fermions. These results indicate a reduction of the fermionic component where the bosonic one is present, in favour of conditions which may be associated to the presence of Bose condensation and Fermi quenching phenomena in nuclear systems. We can find the detailed study of this analysis in [7].

In [8] we focus on probing the Equation Of State (EOS) of asymmetric nuclear matter with $^{40,48}\text{Ca}+^{40,48}\text{Ca}$ collisions at 35 A MeV and more especially on extracting information on the symmetry energy term of the EOS. The observables linked to the symmetry energy are the Isoscaling and the shape of the isotopic distributions. In the framework of the Isoscaling analysis, it was shown that the ratio of the yields Y_i for the same isotope (N, Z) measured in two reactions (1) and (2) is $R_{21}(N, Z) = \frac{Y_2(N, Z)}{Y_1(N, Z)} \approx \exp(\alpha N + \beta Z)$ where C_{sym} is linked to the parameter α via

$$(1) \quad \frac{C_{sym}}{T} = \frac{\alpha/4}{\left(\frac{Z}{\langle A_1(Z) \rangle}\right)^2 - \left(\frac{Z}{\langle A_2(Z) \rangle}\right)^2}.$$

On the other hand, experimentally it is observed that the global isotopic distributions, $K(N, Z)$, combining the yields of fragments obtained in the four systems $^{40,48}\text{Ca}+^{40,48}\text{Ca}$, have a quadratic form. A quadratic approximation of the grand-canonical expression can link the asymmetry energy to the quadratic term of $K(N, Z)$ where: $-\ln Y_i(N, Z) = K(N, Z) = \xi(Z)N + \eta(Z) + \zeta(Z)\frac{(N-Z)^2}{(N+Z)}$ with $\zeta(Z) = C_{sym}(\bar{A}(Z))/T$. So by looking at the isoscaling and experimental isotopic distribution plots we are able to infer the parameter C_{sym}/T in both method and compare them. It turns out that indeed they are very similar, see fig. 6, but now to go further and extract the C_{sym} value itself the knowledge of the excitation energy and temperature T is mandatory and so the secondary decay must be taken into account too. This is done by comparing carefully the experimental data with simulations from AMD and Gemini++. In [8] the importance of surface effects in the evolution of C_{sym}/T has been demonstrated to be very important.

Finally, thanks also to the Indra-VAMOS experimental set-up, we have studied the isospin dependence of the level density parameter in Pd isotopes. We have explored the

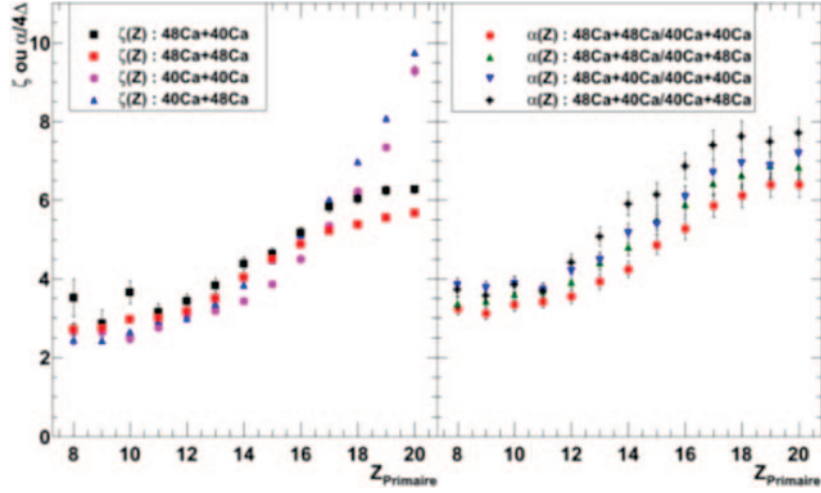


Fig. 6. – Experimental evolution of C_{sym}/T as a function of the charge Z of the reconstructed fragments for two different techniques: Left, extracted from the isotopic distribution information. Right, calculated within the isocalcing approach. Both results are very similar. From [8].

de-excitation properties of hot nuclei formed by fusion reactions with the N/Z from the p drip line to stable nuclei. This has been done by measuring Ar+Ni reactions of judiciously chosen isotopes and incident energy. The idea here is to detect the fusion-evaporation residue into the VAMOS spectrometer (Z, A, E) and the evaporated light particles in coincidence, event by event within the 4π INDRA multidetector. For complete events, by mass conservation, we can thus also have access to the neutron multiplicity so that to completely studied the properties of the compound nucleus in term of cross section, mass asymmetry effects, de-excitation properties (partitions) and, by comparison with model, having clues on the level density parameter. Five Pd isotopes produced by the total fusion of Ar+Ni systems have been obtained $^{92,94,96,100,104}\text{Pd}$ at the same total excitation energy around 2.9 A MeV. Event by event we keep those where each residue is

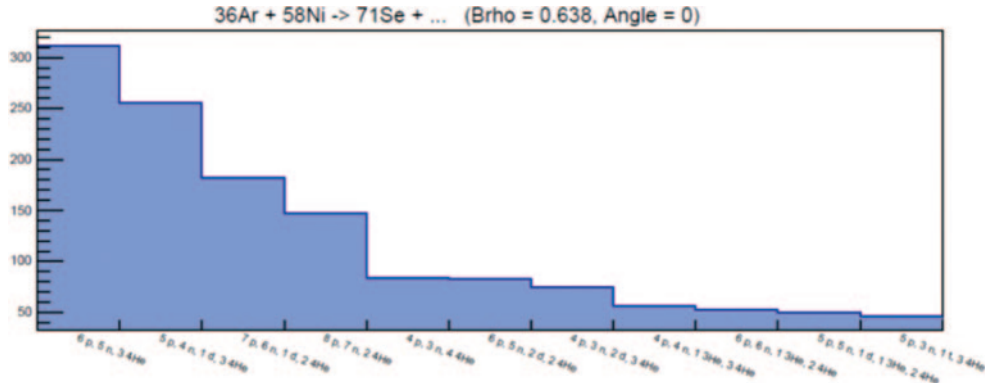


Fig. 7. – The most probable experimental decay channels obtained for the isotope of ^{71}Se residue formed in $^{36}\text{Ar}+^{58}\text{Ni}$ fusion reactions. From [9].

isotopically resolved and the total charge of the full system is achieved. Then we are able for the very first time, to our knowledge, to sort the most probable experimental decay channels for selected isotopes of the residue. See fig. 7 for an example on the ^{71}Se residue. This is a huge constraint for the statistical models but once we are able to reproduce in good agreements the data one can rely better on the model to extract precise values on the thermodynamical properties of the excited fused compound system such as the level density parameter for example. This work is in progress, see [9].

REFERENCES

- [1] INDRA COLLABORATION (LOPEZ O. *et al.*), *Phys. Rev. C*, **90** (2014) 064602.
- [2] INDRA COLLABORATION (MANDUCI L. *et al.*), to be published.
- [3] INDRA COLLABORATION (GRUYER D. *et al.*), *Phys. Rev. C*, **92** (2015) 064606.
- [4] FRANKLAND J. D., these Proceedings.
- [5] INDRA COLLABORATION (BOUGAULT R. *et al.*), *Light charged clusters emitted in 32 MeV/nucleon $^{136,124}\text{Xe}+^{124,112}\text{Sn}$ reactions: chemical equilibrium, ^3He and ^6He production*, in preparation; see also these Proceedings.
- [6] VIENT E., these Proceedings.
- [7] INDRA COLLABORATION (MARINI P. *et al.*), *Phys. Lett. B*, **756** (2016) 194; see also these Proceedings.
- [8] FABLE Q., these Proceedings.
- [9] AUGHEY L., these Proceedings.